THE JOURNAL OF NAVIGATION (2003), **56**, 411–427. © The Royal Institute of Navigation
DOI: 10.1017/S0373463303002388 Printed in the United Kingdom

Simulator Studies on a Collision Avoidance Display that Facilitates Efficient and Precise Assessment of Evasive Manoeuvres in Congested Waterways

Egil Pedersen and Kinzo Inoue

(*Kobe University of Mercantile Marine*)

Masanori Tsugane

(*Japan Marine Science, Inc.*)

This paper is based on two articles by the authors that were published in the March and September 2002 issues of the Journal of Japan Institute of Navigation.

The collision risk to multiple targets and identification of feasible evasive manoeuvres can be assessed simultaneously in true motion by judging the tip of own ship's velocity vector in relation to the display of cone-shaped collision danger regions to acquired targets. Simulator test programmes composed of scenarios with various traffic densities and different speed ranges of own ship have been carried out in order to evaluate the performance of this collision avoidance display versus ARPA (true and relative motion) displays. Experienced navigators and maritime university students with license participated as test subjects. It is shown that the proposed display is capable to facilitate more homogeneous, precise and safe evasive manoeuvres than utilising conventional judgement techniques. The superiority increases with the excess speed of own ship, traffic density and complexity.

KEY WORDS

1. Collision Avoidance. 2. Simulator Studies. 3. Environmental Stress. 4. ARPA Radar.

1. INTRODUCTION. Collisions between encountered ships have the potential to cause the most serious accidents at sea with corresponding human, ecological and economical consequences. Human error is widely regarded as the principal and basic cause of accidents. Safety of ship transit in restricted and congested waterways depends on the mariner's ability to avoid mistakes in judgement and ship-handling processes.

Many of the world's major shipping areas have Traffic Separation Schemes (TSS) or other ship routing systems to separate the traffic flow and thereby minimise the risk of collision (and grounding). Safe navigation in restricted and congested waterways is

https://doi.org/10.1017/S0373463303002388 Published online by Cambridge University Press

further enhanced by Vessel Traffic Services (VTS) systems. Shipboard systems and technologies such as Automatic Radar Plotting Aid (ARPA) systems, Electronic Chart Display and Information Systems (ECDIS) and Automatic Identification Systems (AIS) provide vital information of the surrounding environmental and traffic conditions. Correct and time-efficient interpretation of the monitored traffic condition depends on the mariner's ability to properly process the collision avoidance information available. Heavy traffic conditions can easily impose a workload to the mariner, which represents an increased risk of misjudgement and mistakes occurring. The time factor in particular is critical to the High Speed Craft (HSC) mariner in order to make necessary target identification and to assess the risk of collision, and this can be greatly compressed. A particularly essential factor is the human-machine interface of collision avoidance systems as the human ability to process significant amounts of (alpha-numeric) data is limited.

Lenart (1983) showed theoretically that a cone-shaped collision danger region can be displayed to an acquired target in true vector mode by considering the relative motion between own ship and a target for a constant minimum distance at Closest Point of Approach (*CPA*). The size and position of the region are independent of own ship's motion parameters and can therefore be displayed to any acquired target. The collision region is to be interpreted with respect to the tip of own ship's velocity vector and enables the mariner to judge collision avoidance to multiple targets in true motion, and simultaneously identify feasible evasive manoeuvres.

This paper shows a geometrical approach to the collision problem at sea that leads to derivation of collision danger lines and sectors in accordance with Lenart (1983). The main results of two simulator test programmes (Pedersen *et al*., 2002a and 2002b) are presented and discussed. Fifteen subjects, captains and maritime university students with licenses, participated in the first programme that concerned various traffic densities in restricted waters with own ship employed as a conventional speed vessel. The evaluation of the performances was based on application of the Environmental Stress (ES) model (Inoue, 2000) which is a quantitative model for evaluating the difficulty of ship handling in restricted and congested shipping areas. A second test programme concerned HSC navigation in congested waterways with the participation of 8 subjects of which 4 were HSC navigators.

The simulator studies showed that the subjects judging collision avoidance based on the display of cone-shaped collision danger regions in true motion performed more homogeneous, safe and precise manoeuvres than those utilising ARPA (true and relative motion) displays. The superiority increases with the excess speed of own ship and with traffic density and complexity. The easily understandable interpretation of collision risk to multiple targets and identification of feasible evasive action in true motion suggests that the proposed visualisation-based anti-collision display should have the potential to become widely accepted by mariners.

2. ANTI-COLLISION ASSESSMENT IN TRUE MOTION.

Consider two vessels (own ship and an external target) travelling on a plane sea surface in an earth-fixed x–y Cartesian co-ordinate system. Let $\mathbf{X_0}(\mathrm{L}) = [X_0\ Y_0]^{\mathrm{T}}$ and $\mathbf{X_T}(\mathrm{L}) = [X_{\mathrm{T}}\ Y_{\mathrm{T}}]^{\mathrm{T}}$ be the position vectors of own ship and target, respectively, $\mathbf{V_0}(\mathrm{LT}^{-1}) = [V_{0\mathrm{x}}\ V_{0\mathrm{y}}]^{\mathrm{T}}$ and $\mathbf{V_T}(\mathrm{LT}^{-1}) = [V_{\mathrm{Tx}}\ V_{\mathrm{Ty}}]^{\mathrm{T}}$ represent the corresponding true velocity vectors, and let ψ_0 and ψ_{T} represent the respective true courses. Furthermore, $t(\mathrm{T})$

https://doi.org/10.1017/S0373463303002388 Published online by Cambridge University Press

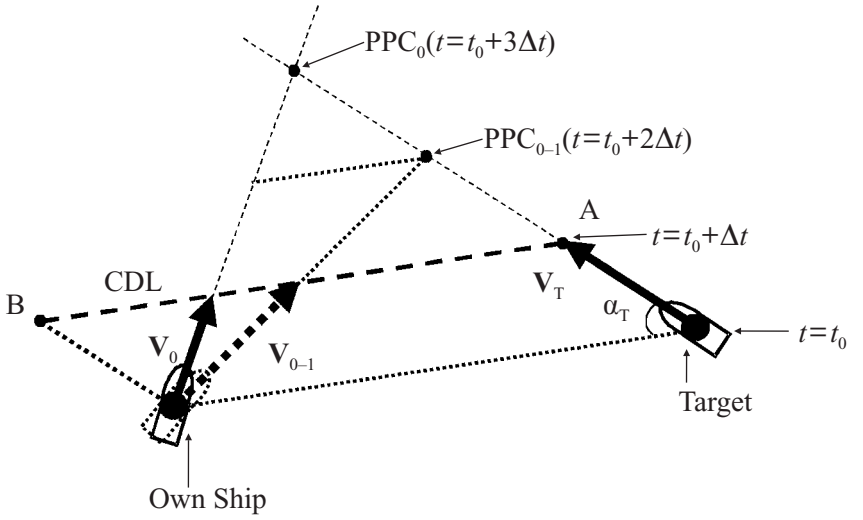


Figure 1. Own ship ($\mathbf{V_0}$ or $\mathbf{V}_{0-1}$) and target ($\mathbf{V}_T$) on collision course(s).

is time with t_0 as the present (reference) time, Δt(T) is equivalent with the vector length in time scale, and α is the aspect angle (relative bearing).

2.1. *Geometrical Interpretation of Velocity Vectors.* Consider the two vessels approaching each other in a way that will eventually cause collision if speed and course are maintained (see Figure 1). The vessels have a Potential Point of Collision (PPC) at $t(=TCPA)=t_0+3\Delta t$ if the motion parameters according to $\mathbf{V_0}$ and $\mathbf{V}_T$ are unchanged. The mathematical condition for collision can be formulated as $V_0 \sin\alpha_0 = V_T \sin\alpha_T$, with V_0 and V_T as the scalar values of the respective velocity vectors. It follows that the PPC can be moved to $t=t_0+2\Delta t$ on the target's track line if $\mathbf{V_0}$ is altered to $\mathbf{V}_{0-1}$, i.e. $V_{0-1}\sin\alpha_{0-1} = V_T \sin\alpha_T$. Thus, any manoeuvre that deflects the end of own ship's velocity vector away from the bold dashed line is a potential collision avoidance manoeuvre. The dashed line can therefore be regarded as a Collision Danger Line (CDL). It is simply created by parallel displacement of the bearing line to the target, a distance equal to the length of $\mathbf{V}_T$, and is therefore independent of own ship's motion parameters. The dotted line from the centre of own ship, parallel to $\mathbf{V}_T$, represents the course of own ship that would result in parallel movement. The interception point (B) between this line and the CDL can therefore be regarded as a limit for relevant anti-collision evaluation.

The CDL is then determined by the position vectors $\mathbf{X}_A(L)=[X_A\ Y_A]^T$ and $\mathbf{X}_B(L)=[X_B\ Y_B]^T$ which can be expressed as,

$$\mathbf{X}_A = \mathbf{X}_T + V_T \Delta t \mathbf{I} \Psi_T,$$

and

$$\mathbf{X}_B = \mathbf{X_0} + V_T \Delta t \mathbf{I} \Psi_T,$$

where $\mathbf{\Psi}_T = [\sin\psi_T \cos\psi_T]^T$ for $0 \leqslant \psi_T \leqslant 2\pi$ and I is the 2×2 unit matrix.

The general solution of the collision scenario studied is obtained when considering a minimum passing distance (*CPA* limit). Figure 2 shows a cone-shaped collision region (dashed lines) as it can be imagined on a standard ARPA in relative motion

https://doi.org/10.1017/S0373463303002388 Published online by Cambridge University Press

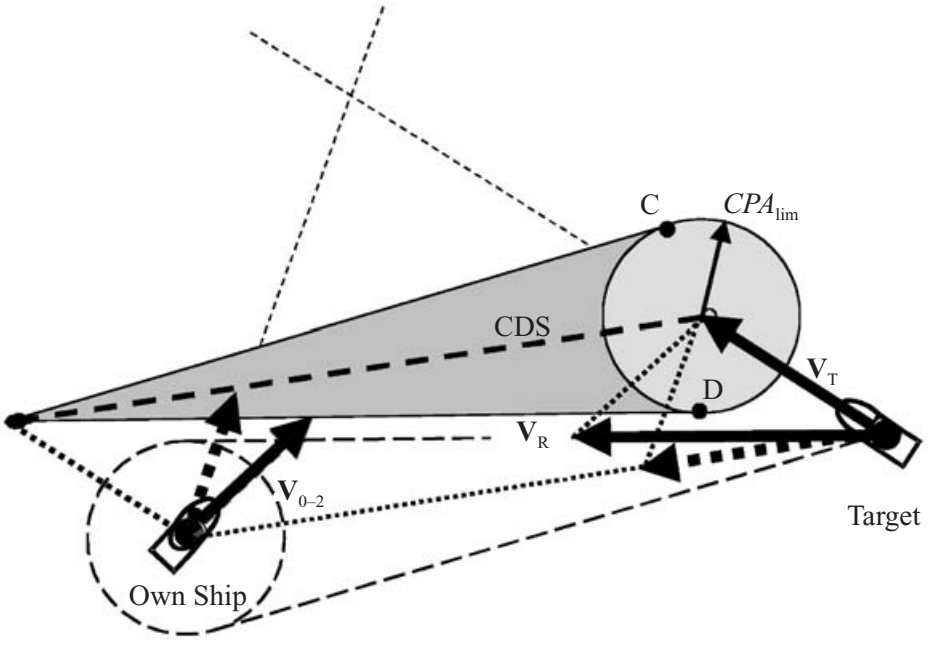


Figure 2. Cone-shaped collision danger regions as they appear in true (shadowed sector) and relative (dashed sector) motion displays.

display from the viewpoint of own ship. A *CPA* limit circle is located at the centre of own ship, for example by utilising the Variable Range Marker.

The solution to pass at a minimum safe distance astern of the target is shown by a course change $\mathbf{V}_{0-2}$ to starboard, which deflects the relative vector $\mathbf{V}_R$ so its extension becomes a tangent to the *CPA* limit circle. Figure 2 illustrates how the imagined cone-shaped collision region in the relative display can be transformed to appear in the true motion display (shadowed sector). This region is hereinafter referred to as the Collision Danger Sector (CDS).

The co-ordinates (C and D) for the tangents to the *CPA* limit circle are dependent on the orientation of the CDL. The corresponding position vectors $\mathbf{X}_C(L)=[X_C\ Y_C]^T$ and $\mathbf{X}_D(L)=[X_D\ Y_D]^T$ can be formulated as,

$$\mathbf{X}_C=\mathbf{X}_B+(|\mathbf{X}_A-\mathbf{X}_B|^2-CPA_{lim}^2)^{\frac{1}{2}}\Omega_T,$$

and

$$\mathbf{X}_D=\mathbf{X}_B+(|\mathbf{X}_A-\mathbf{X}_B|^2-CPA_{lim}^2)^{\frac{1}{2}}\Phi_T,$$

where $CPA_{lim}(L)$ is the selected limit of passing distance at closest point of approach, and $\mathbf{\Omega}_T=[(-1)^j\cos(\gamma+(-1)^k\beta)\ \ (-1)^m\sin(\gamma+(-1)^k\beta)]^T$, $\mathbf{\Phi}_T=[(-1)^j\cos(\gamma+(-1)^n\beta)\ \ (-1)^m\sin(\gamma+(-1)^n\beta)]^T$. Here, $\gamma=|\tan^{-1}[(Y_A-Y_B)/(X_A-X_B)]|$ if $X_A\neq X_B$; $\gamma=\pi/2$ for $X_A=X_B$, and $\beta=\sin^{-1}[CPA_{lim}/|\mathbf{X}_A-\mathbf{X}_B|]$ if $CPA_{lim}<|\mathbf{X}_A-\mathbf{X}_B|$, else only CDL to be displayed. j, k, m and n are integers (0 or 1) according to the scheme; $Y_A\geqslant Y_B$ and $X_A\geqslant X_B$: $[j, k, m, n]=[0, 1, 0, 0]$, $Y_A\geqslant Y_B$ and $X_A<X_B$: $[j, k, m, n]=[1, 1, 0, 0]$, $Y_A<Y_B$ and $X_A\geqslant X_B$: $[j, k, m, n]=[0, 0, 1, 1]$, $Y_A<Y_B$ and $X_A<X_B$: $[j, k, m, n]=[1, 0, 1, 1]$.

https://doi.org/10.1017/S0373463303002388 Published online by Cambridge University Press

The position of own ship's vector in relation to the displayed collision danger line and sector shows the severity of the collision threat simultaneously with the possibility of avoidance by changing course and/or speed. There is a direct collision threat if the tip of own ship's vector reaches the CDL ($CPA_{\text{lim}}=0$). If the tip of the vector is at the edge of the CDS, own ship will pass a distance equal to the set CPA limit either ahead, or astern, of the target. Any real or imagined manoeuvre, which deflects the end of own ship's vector out of the CDS, will be a potential evasive manoeuvre.

2.2. *Theoretical Analysis of the Relative Motion for* $\partial/\partial t(CPA)=0$ (*Lenart,* 1983). CPA is found by studying the differential of relative distance with respect to time t,

$$CPA=\left|\frac{(X_{\text{T}}-X_0)V_{\text{Ry}}-(Y_{\text{T}}-Y_0)V_{\text{Rx}}}{V_{\text{R}}}\right|.$$

If both sides of the equation are squared, and the velocity components are inserted for V_{R}, the following equation related to the relative velocity components can be obtained:

$$\frac{V_{\text{Ry}}}{V_{\text{Rx}}}=\frac{(X_{\text{T}}-X_0)(Y_{\text{T}}-Y_0)\pm CPA\sqrt{(X_{\text{T}}-X_0)^2+(Y_{\text{T}}-Y_0)^2-CPA^2}}{(X_{\text{T}}-X_0)^2-CPA^2},$$

which states that the ratio is constant provided CPA is constant. The equation always has two real roots if the present distance to the target is greater than, or equal to, the distance at closest approach. By substituting the vector relationship $\mathbf{V}_{\text{R}}(\text{LT}^{-1})=\mathbf{V}_{\text{T}}-\mathbf{V}_0$ it follows that own ship's speed versus course can be written in the form,

$$V_0(\psi_0)=\frac{(V_{\text{Ry}}/V_{\text{Rx}})V_{\text{Tx}}-V_{\text{Ty}}}{(V_{\text{Ry}}/V_{\text{Rx}})\sin\psi_0-\cos\psi_0}.$$

The lines on the (V_0, ψ_0) plane intersect at the point where own ship's motion parameters are identical to those of the target, irrespective of CPA. $V_0(\psi_0)$ can be plotted by applying a scaling factor $\tau(\text{T})$ to the velocity co-ordinates such that $x(\text{L})=(V_0\sin\psi_0)\tau$ and $y(\text{L})=(V_0\cos\psi_0)\tau$. The formulation then becomes

$$y(\tau)=(V_{\text{Ry}}/V_{\text{Rx}})x(\tau)-((V_{\text{Ry}}/V_{\text{Rx}})V_{\text{Tx}}-V_{\text{Ty}})\tau,$$

which is a linear equation and can be used to draw two lines for each selected CPA limit. The area within these lines represents a cone-shaped collision region, Figure 3.

3. THE ENVIRONMENTAL STRESS MODEL.

Inoue (2000) introduced the Environmental Stress (ES) model as a quantitative model for evaluating the difficulty of ship handling caused by restricted manoeuvring area and traffic congestion. The environmental elements that are taken into account in the ES model are:

a) Topographical conditions (e.g. land, breakwaters, buoys, moored ships).
b) Traffic conditions (traffic flow and other vessels).
c) External disturbance conditions (e.g. winds and currents).

https://doi.org/10.1017/S0373463303002388 Published online by Cambridge University Press

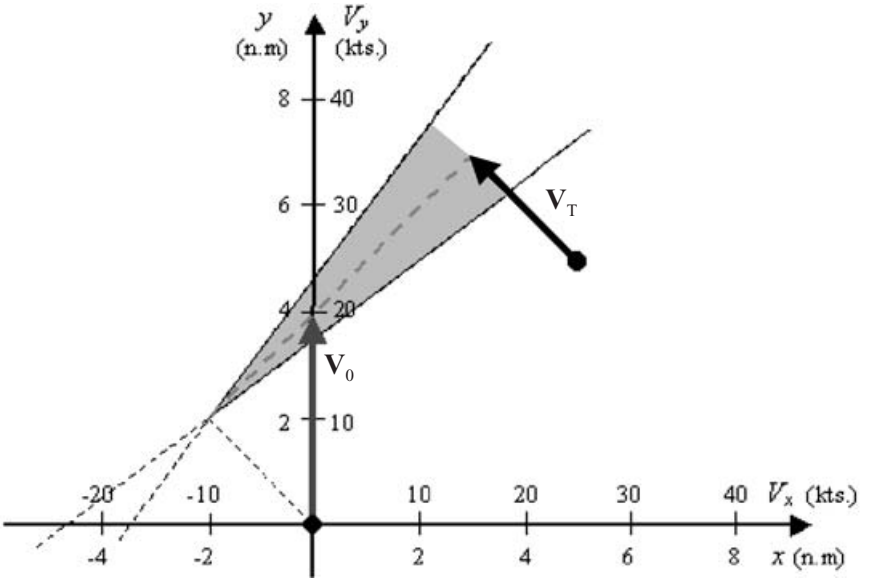


Figure 3. The collision region (shadowed area) for a single target: τ(hrs) = 0·2, CPA_{lim}(nm) = 1·0, $\mathbf{X_0}$(nm) = $[0\ 0]^T$, $\mathbf{X_T}$(nm) = $[5\ 5]^T$, $\mathbf{V_0}$(kts) = $[0\ 20]^T$, $\mathbf{V_T}$(kts) = $[-10\ 10]^T$, (Lenart, 1983).

The model structure is composed of the following parts:

1) Evaluation of ship handling difficulty arising from restrictions to the water area available for manoeuvring; a quantitative index expressing the degree of stress forced on the mariner by topographical restrictions (ES_L value) is calculated on the basis of the time to collision (TTC) with any obstacles.
2) Evaluation of ship handling difficulty arising from restrictions to make collision avoidance manoeuvres; a quantitative index expressing the degree of stress forced on the mariner by traffic congestion (ES_S value) is calculated on the basis of the TTC with any external ships.
3) Aggregate evaluation of ship handling difficulty due to both the topographical and traffic environments; the stress value (ES_A value) is derived by superimposing the ES_L and ES_S values. In open waters, with no manoeuvring restriction or targets, the mariner feels no stress and difficulty in ship handling as there is sufficient TTC regardless of the direction in which the ship proceeds. In narrow waterways, and with the presence of targets, the TTC is restricted and the mariner feels stress and difficulty with ship handling.

The ES values are calculated according to the following procedure:

1) Consider the ship's course within a sector of 180° centred on the present course.
2) Calculate TTC for each degree gradation in the range of $+/-90°$.
3) Convert TTC into the mariner's perception of safety for each degree by the conversion formula;

$$SJ_L,\ SJ_S = \alpha TTC + \beta,$$

https://doi.org/10.1017/S0373463303002388 Published online by Cambridge University Press

Table 1. The relation between the mariner's subjective judgement, *ES* value, stress ranking and acceptance criteria. The maximum stress value possible is 1000, while values below 500 are regarded as negligible/marginal stress. (Inoue, 2000.)

Mariner's Subjective Judgement	*ES* Value	Stress Ranking	Acceptance Criteria
0 Extremely Safe	0	Negligible	Acceptable
1 Fairly Safe			
2 Somewhat Safe			
3 Neither Safe/Dangerous	500	Marginal	
4 Somewhat Dangerous	750	Critical	Unacceptable
5 Fairly Dangerous	900		
6 Extremely Dangerous	1000	Catastrophic	

which is given by regression equations found through simulator experiments and questionnaire (Inoue *et al.*, 1998). SJ_L and SJ_S are the mariners Subjective Judgement in relation to *TTC* with obstacles and targets, respectively, with the scales consisting of numerical values from 0 (most safe) to 6 (most dangerous). Table 1 gives the relation between the mariner's subjective judgement, *ES* value, stress ranking and acceptance criteria. α and β are coefficients determined by the size of own ship in case of SJ_L value or by combination of the size of own ship and target in case of SJ_S value.

4) Summarise the *SJ* values within the sector of $+/-90^\circ$ about own ship's course to find the stress values by

$$ES_L = \sum_{i=-90^\circ}^{+90^\circ} [SJ_L]_i,$$

$$ES_S = \sum_{i=-90^\circ}^{+90^\circ} [SJ_S]_i.$$

If there is no danger in all directions the *SJ* value equals 0 over 180°, i.e. $0 \times 180 = 0$ is assigned the minimum *ES* value possible. If there is immediate danger, regardless of the ship's direction, the *SJ* value $= 6$ extends over 180°, i.e. $6 \times 180 \equiv 1000$ is assigned the maximum *ES* value.

4. SIMULATOR TEST PROGRAMMES.

Simulator test programmes have been carried out on the ship handling simulator facility of Kobe University of Mercantile Marine. The geometrical solution of collision danger lines and sectors was implemented as a display option on the particular ARPA and is hereinafter referred to as the Collision Danger Presentation (CDP) display.

4.1. *Apparatus.* The mock-up of a ship's bridge was installed with observation distance of about 5 m and was instrumented with pilot stand, operation console and a radar image with basic ARPA functions (ex. Trial Manoeuvre option that was not implemented on the particular facility). An assessment monitor display with graphics in real time showing the difficulty in ship handling by the ES model was also installed.

https://doi.org/10.1017/S0373463303002388 Published online by Cambridge University Press

Table 2. Own ship and target data for the uncomplicated and complicated traffic scenarios at initial position.

	Uncomplicated traffic scenario			Complicated traffic scenario		
	Initial Range/ Bearing [nm]/[deg]	Initial Course/ Speed [deg]/[kts]	Initial *CPA*/*TCPA* [nm]/[min]	Initial Range/ Bearing [nm]/[deg]	Initial Course/ Speed [deg]/[kts]	Initial *CPA*/*TCPA* [nm]/[min]
O. S	—/—	000/10·0	—/—	—/—	000/12·0	—/—
1	8·3/352	162/8·0	0·0/28	1·9/274	045/16·0	0·0/10
2	7·2/031	260/7·0	0·0/33	3·9/342	135/8·0	0·0/12·5
3				7·0/000	180/16·0	0·0/15
4				8·8/024	225/12·0	0·2/24
5				3·9/080	315/14·4	0·0/23

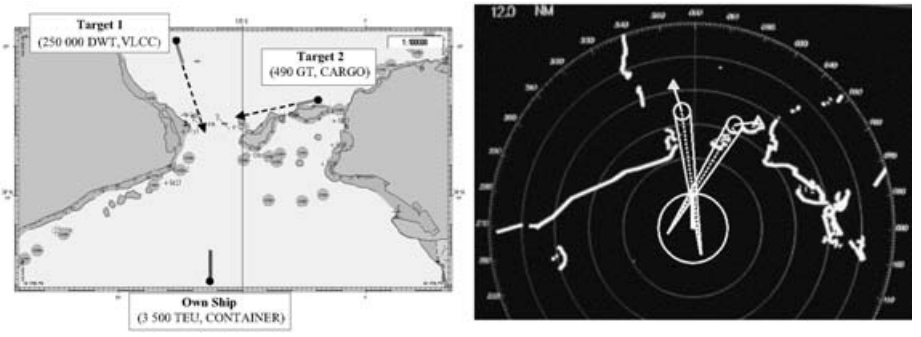


Figure 4. Uncomplicated traffic scenario: Initial position and velocity vector of own ship and the targets (left figure). CDP display at initial position (right figure). (Radar range = 12 nm, vector length = 12 minutes, *CPA* limit = 0·5 nm.)

4.2. *Participants.* 10 final-year maritime students with license and 9 experienced navigators participated as subjects. The experienced subjects were 5 Captains of the NYK Line and 4 Captains of the company operating the K-Jet hydrofoil crafts.

4.3. *Conventional-speed Scenarios.* Scenarios with various traffic densities and difficulties were carried out in Tomogashima Suidō, which is about 2 nm wide at its narrowest part at the south entrance of Osaka Bay. Own ship was a 3500 TEU container ship operating at 10 or 12 knots speed and was initially located about 5 n. miles south of Tomogashima Suidō and heading north (000°). Other ships were encountered in succession from port and starboard sides and/or head-on. All targets kept constant speed and course. A daylight scene was created with landscape and vessels visible. The environmental conditions were clear visibility with no wind or current.

Table 2 shows the details of traffic set-up for the uncomplicated and complicated traffic scenarios in question. The base position ($x = 0$, $y = 0$) was N 34° 20·0′ E 135° 00·0′ from which own ship initially was located at (-1750, $-15\,149$) m and (-1750, $-14\,454$) m, respectively, for the two scenarios presented. Figures 4 and 5 show the initial position and velocity vector of own ship and targets and the CDP display activated at initial position for the scenarios. A circle, representing the length of own ship's velocity vector, is located at the centre to help determining an evasive

https://doi.org/10.1017/S0373463303002388 Published online by Cambridge University Press

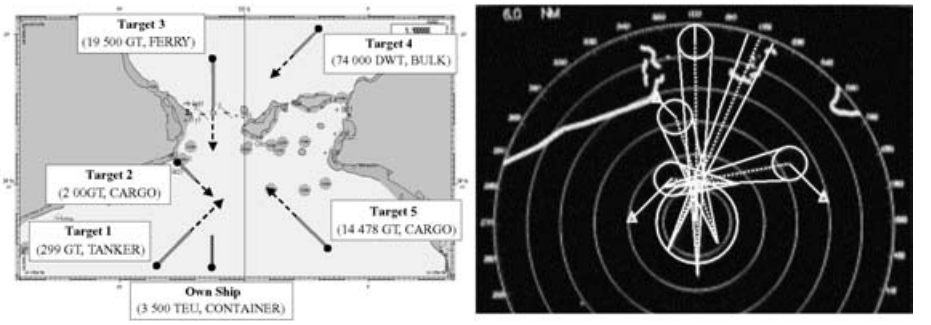


Figure 5. Complicated traffic scenario: Initial position and velocity vector of own ship and targets (left figure). CDP display at initial position (right figure). (Radar range = 6 nm, vector length = 6 minutes, *CPA* limit = 0·5 nm.)

manoeuvre by change of course. (Nautical charts were provided by OceanView™, C-Map Norway AS.)

4.4. *High-speed Scenarios*. Scenarios with own ship as an HSC were carried out in heavy traffic congestion between Kobe and Kansai International Airport. Own ship employed was the K-Jet hydrofoil craft operating with a nominal speed of 45 knots. Other ships were encountered in succession from port and starboard sides according to the most commonly used ship traffic routes in this sector of Osaka Bay. All targets kept constant speed and course. A daylight scene with restricted visibility of 0·5 n. miles was created. The environmental conditions were no wind or current.

Table 3 shows the details of traffic set-up for the scenarios. (Bold figures represent changes in traffic set-up prior between student and experienced subjects.) Figures 6 through 8 show the available ARPA and CDP displays at the position from which own ship was allowed to make a course-evasive manoeuvre, i.e. 120 sec from initial time. The base position ($x = 0$, $y = 0$) of the scenarios was N 34° 40·25′ E 135° 10·25′.

4.5. *Procedures*. For the conventional-speed scenarios a total of 15 subjects, 10 students and the 5 NYK Captains, participated and were separated into three equal-sized groups. One of the student groups was appointed reference group and performed anti-collision assessment based on the available ARPA (true and relative motion) displays while the two other groups utilised CDP display only. Eight subjects participated in the high-speed scenarios that took place several months later of which 4 subjects were experienced K-Jet navigators. The 8 subjects were to utilise the respective CDP and preferred ARPA displays on each scenario, but on separate runs. The subjects were not informed that each scenario was to be run twice. To further counteract learning trends of the monitored traffic condition in the high-speed scenarios, the order in which the CDP or ARPA displays should be utilised was randomised for each subject.

The subjects were numbered alphabetically according to their schedule on the simulator. Those to utilise the CDP display were made familiarised with the principles in an introductory session. This was followed by brief practice trials on the simulator.

All targets were pre-acquired prior to starting a scenario. Each subject was informed that other ships would keep constant motion parameters. Normal safety and navigation rules with respect to the monitored targets and topographies had to be

https://doi.org/10.1017/S0373463303002388 Published online by Cambridge University Press

Table 3. Own ship (K-Jet hydrofoil craft) and target data for the Kobe–Kansai and Kansai–Kobe scenarios at initial position.

Kobe–Kansai			Kansai–Kobe		
Type of Vessel	Initial Position X [m], Y [m]	Initial Course/ Speed [deg]/[kts]	Type of Vessel	Initial Position X [m], Y [m]	Initial Course/ Speed [deg]/[kts]
K-Jet (O. S)	9723, −5043	180/45	K-Jet (O. S)	10 093, −27 427	000/45
Cargo 499 GT	11 713, −11 999	276/13	BC 74k DWT	8612, −21 164	050/11(**12**)
BC 74k DWT	13 890, −12 574	275/15	CC 3500 TEU	6189, −21 637	050/17
CC 3500 TEU	12 686, −13 554	227/16	Cargo 5k DWT	7871, −14 673	095/8
Cargo 5k DWT	11 101, −15 713	230/14	Tank 299 GT	3797, −10 867	082/13
BC 74k DWT	6605, −23 318	049/13	Ferry	7032, −9942	083/12(**13**)
Fishing boat	3797, −23 625	107/12	Fishing boat	17 133, −4398	262/12
Fishing boat	845, −22 586	108/12	Ferry	16 078, −5294	262/15
Tank 299 GT	7498, −21 072	050/13	BC 74k DWT	14 911, −12 516	275/13
CC 3500 TEU	4547, −14 813	095/14	Fishing boat	17 131, −13 330	275/13
Heavy Lifter	6575, −14 673	092/14	Heavy Lifter	11 945, −14 450	228/14
Cargo 499 GT	15 922, −11 759	275/13	Ferry	10 352, −20 508	050/13(**14**)
Heavy Lifter	2756, −16 035	095/16	LNGC	9565, −14 207	095/10
CC 3500 TEU	15 725, −12 490	228/16	PCC 3500	13 616, −13 700	230/15
				13 354, −13 886	
CC 3500 TEU	10 069, −9817	275/16	Fishing boat	13 616, −4811	262/13
Tank 6k DWT	8439, −10 548	275/14	BC 74k DWT	9311, −19 618	051/14(**15**)
LNGC	2025, −13 727	095/15	RORO	12 828, −11 900	276/13
Cargo 499 GT	9846, −15 501	228/16	LNGC	5683, −9593	082/12
PCC 3500	4895, −23 180	049/13	**Heavy Lifter**	**10 942, −16 639**	**226/12**
			BC 70k DWT	**9170, −17 032**	**228/12**
			LNGC	**5851, −13 981**	**095/12**

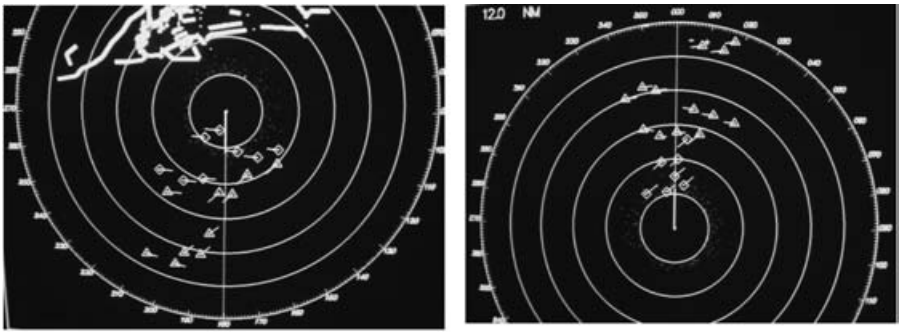


Figure 6. True motion displays for Kobe–Kansai (left) and Kansai–Kobe (right) scenarios. (Radar range = 12 nm, vector length = 1 minute.)

followed. The subjects were required to keep a minimum passing distance (*CPA* limit) of 0·5 n. miles to all targets in the conventional-speed scenarios and 0·3 n. miles to all targets in the high-speed scenarios. In the latter it was also required to maintain minimum deviation from original track line. All subjects were able to perform the experimental trials, but candidate A in the high-speed test programme could not attend the final part of the schedule.

https://doi.org/10.1017/S0373463303002388 Published online by Cambridge University Press

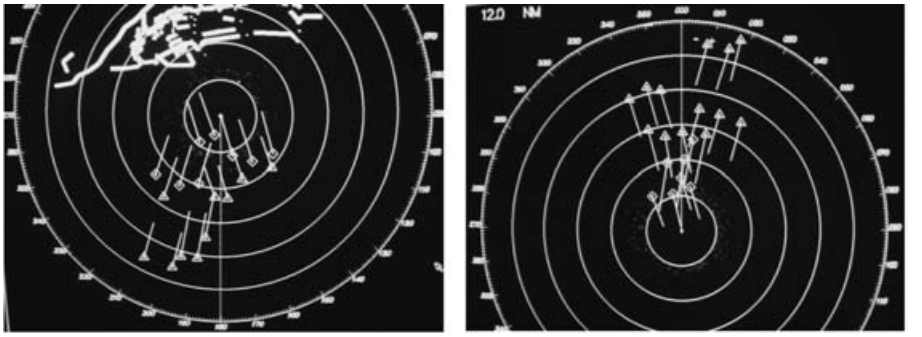


Figure 7. Relative motion displays for Kobe–Kansai (left) and Kansai–Kobe (right) scenarios. (Radar range = 12 nm, vector length = 1 minute.)

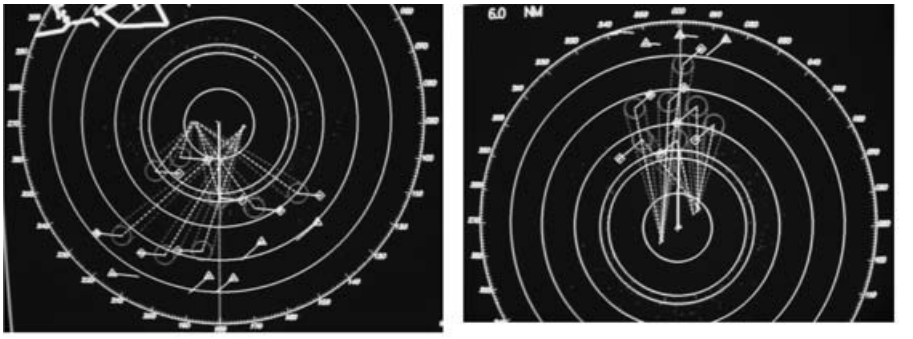


Figure 8. CDP displays for Kobe–Kansai (left) and Kansai–Kobe (right) scenarios. (Radar range = 6 nm, vector length = 1 minute, *CPA* limit = 0·3 nm.) Collision lines and sectors displayed if $0 < TCPA_{\text{Target } i} < TCPA$ limit (set to 6 minutes, $i = 1, \ldots, N$).

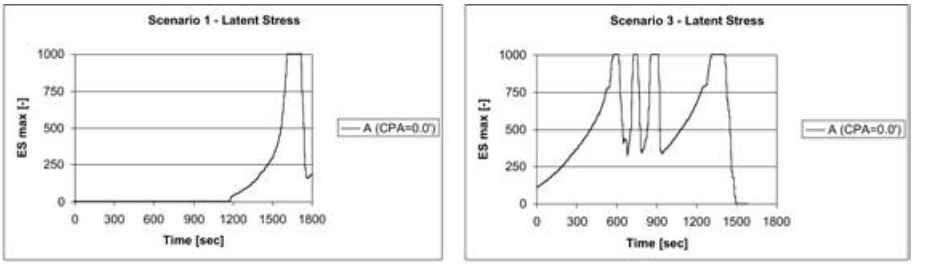


Figure 9. Latent stress in the uncomplicated (left) and complicated (right) conventional-speed scenarios due to external targets.

5. RESULTS. Figure 9 shows the latent stress (ES_S value) that was put to the subjects due to external targets for the conventional-speed scenarios when own ship sails without any evasive manoeuvres. The results of subjects evasive manoeuvring are shown in Figures 10 through 15 and are presented as the aggregated (max.) stress value *vs.* time, own ship's track and minimum *CPA* for the subjects in each group and scenario.

https://doi.org/10.1017/S0373463303002388 Published online by Cambridge University Press

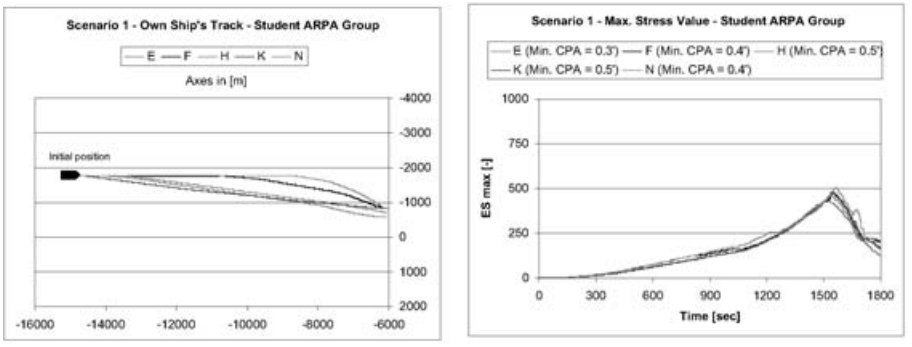


Figure 10. Conventional-speed scenario (Uncomplicated traffic): Track of own ship (left) and max stress values and min *CPA* (right) for the Student ARPA Group.

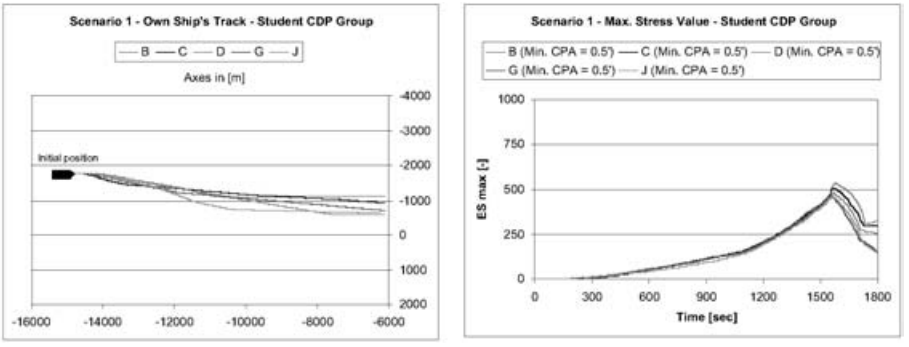


Figure 11. Conventional-speed scenario (Uncomplicated traffic): Track of own ship (left) and max stress values and min *CPA* (right) for the Student CDP Group.

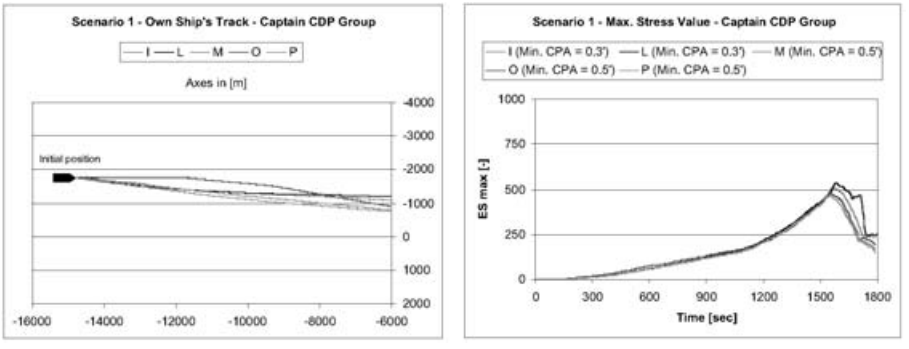


Figure 12. Conventional-speed scenario (Uncomplicated traffic): Track of own ship (left) and max stress values and min *CPA* (right) for the Captain CDP Group.

Figures 16 through 19 show the own ship's track and minimum passing distance to the closest target for the individual subject in each scenario and number of targets with minimum *CPA* violating the required *CPA* limit in the high-speed test programme.

https://doi.org/10.1017/S0373463303002388 Published online by Cambridge University Press

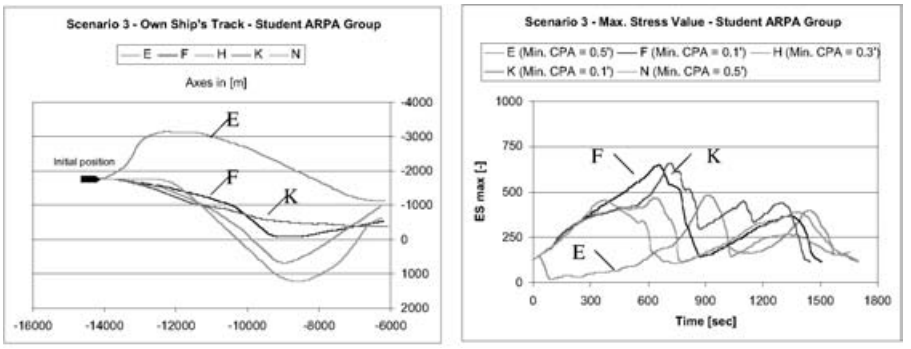


Figure 13. Conventional-speed scenario (Complicated traffic): Track of own ship (left) and max stress values and min *CPA* (right) for the Student ARPA Group.

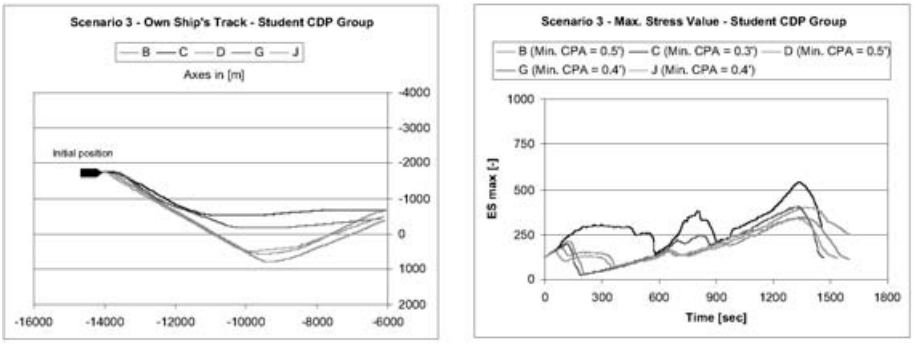


Figure 14. Conventional-speed scenario (Complicated traffic): Track of own ship (left) and max stress values and min *CPA* (right) for the Student CDP Group.

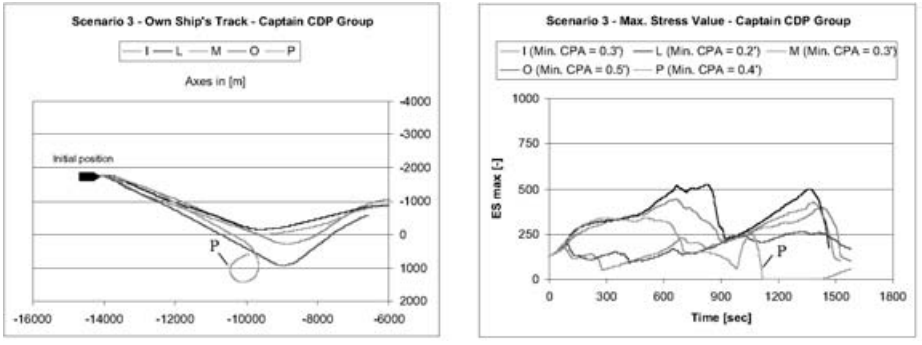


Figure 15. Conventional-speed scenario (Complicated traffic): Track of own ship (left) and max stress values and min *CPA* (right) for the Captain CDP Group.

6. DISCUSSION. The conventional-speed scenario with uncomplicated traffic condition did not represent any major difficulties for the judgement process. Figures 10 through 12 show that the maximum stress (*ES*) value for all subjects were in the range of 450–550, which reflects low stress, and there is no significant

https://doi.org/10.1017/S0373463303002388 Published online by Cambridge University Press

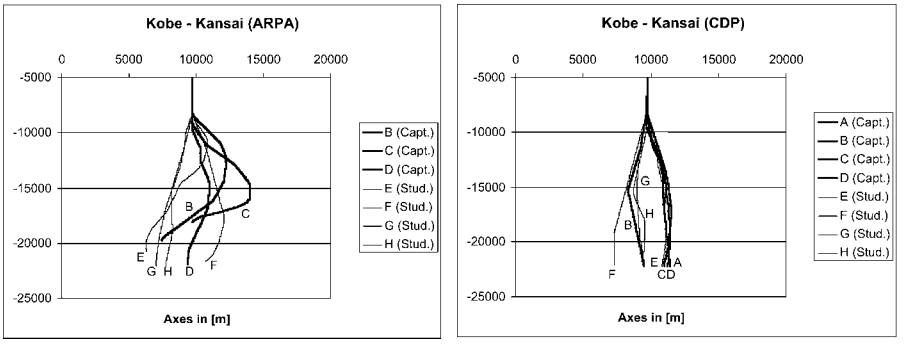


Figure 16. High-speed scenario (Kobe–Kansai): Track of own ship due to judgement based on ARPA display (left) and CDP display (right).

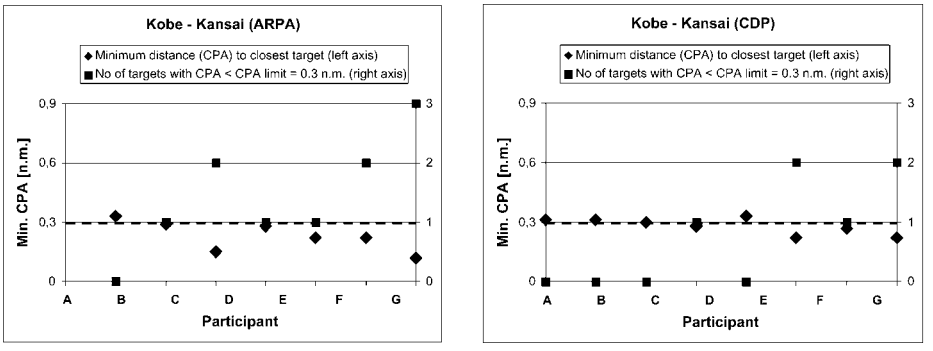


Figure 17. High-speed scenario (Kobe–Kansai): Minimum *CPA* to closest target and number of targets violating the required *CPA* limit (0·3 nm) for judgement based on ARPA display (left) and CDP display (right).

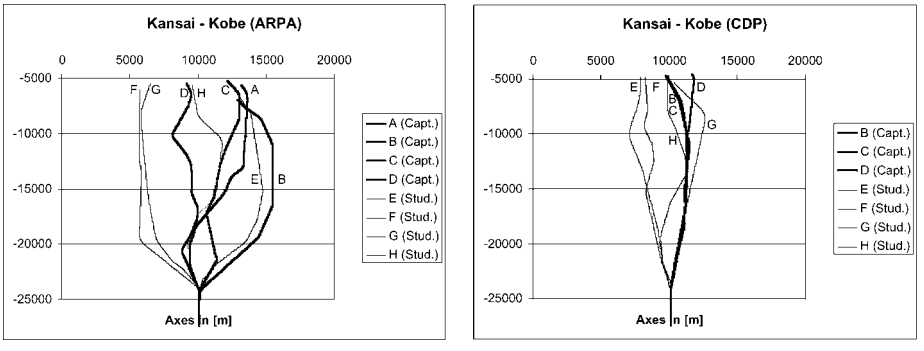


Figure 18. High-speed scenario (Kansai–Kobe): Track of own ship due to judgement based on ARPA display (left) and CDP display (right).

difference in the performance between the groups. However, it is noticeable that the majority of the subjects in the CDP groups maintained the required minimum safety distance of 0·5 nm and also carried out slightly more homogeneous manoeuvres than the ARPA group of students.

https://doi.org/10.1017/S0373463303002388 Published online by Cambridge University Press

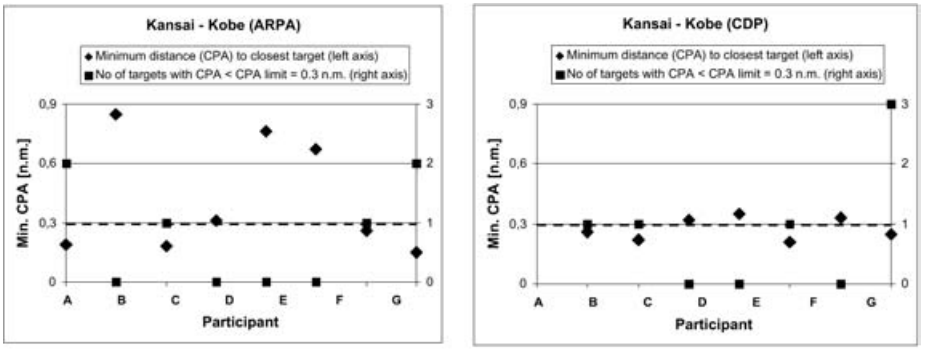


Figure 19. High-speed scenario (Kansai–Kobe): Minimum *CPA* to closest target and number of targets violating the required *CPA* limit (0·3 nm) for judgement based on ARPA display (left) and CDP display (right).

The complicated traffic conditions scenario was constructed with 4 of the 5 targets on direct collision course with own ship. This scenario forced the subjects to make early decision-making (Fig. 9) and revealed considerable variations in the ability to make proper evasive manoeuvre decisions between the two groups utilising CDP display and the subjects utilising conventional judgement. The CDP groups could identify that an initial course change to starboard of about 30° (Fig. 5) would be a possible solution to achieve a *CPA* of 0·5 nm. Figures 13 through 15 show a clear trend that the CDP groups made the initial evasive manoeuvre significantly more quickly and distinctly than the reference group of students. Subject E in the reference group passed the encountered traffic by a course change to port while two other (F and K) eventually came close to the crossing tanker (min. $CPA = 0{\cdot}1$ n. miles) with *ES* values approaching the unacceptable acceptance criteria level range. The scenario's difficulty can also be illustrated (Fig. 15) by the 360° turn carried out by one of the Captains (P) who felt uncomfortable with the decreasing distance to land.

The results of the high-speed scenarios (Figs 16–19) revealed that the CDP display's superiority increases with the excess speed of own ship and with traffic density. The individual subjects selected, in general, course changes with minimum deviations from original track line in order to obtain the required safety distance when judging collision avoidance based on the CDP display. The performance when using preferred ARPA display (true motion) showed large individual variations in course setting.

On the negative side with CDP display it was noticeable that some subjects misunderstood the importance of reducing the vector length with decreasing relative distances to be able to supervise the collision risk until passing the closest target(s). This failure caused the subjects in question to make evasive manoeuvres in relation to more distant targets, thus violating the required minimum passing distance (0·3 nm) to the closest target(s). It should also be pointed out that some subjects showed that they were tempted to make frequent and minor course alterations that are difficult to detect by other ships and might be contrary to the requirements of the COLREGS, when the display showed a gap in the traffic. These failures are probably associated with the short practical training time (10–15 minutes) for each subject prior to carrying out the scenarios.

An additional feature of the method is that there are neither limitations to what target in an acquired traffic scenario from which collision risk can be assessed, nor

https://doi.org/10.1017/S0373463303002388 Published online by Cambridge University Press

any restrictions to how target position and motion data are generated. Pedersen and Jacobsen (2002) argued that the concept can therefore be applied for marine traffic surveillance purposes (like VTS systems) and linked to Electronic Chart Display and Information Systems (ECDIS) and Automatic Identification Systems (AIS).

7. CONCLUSIONS. Cone-shaped collision danger regions that are independent of own ship's motion parameters can be displayed to acquired targets in true motion. By inspecting the tip of own ship's velocity vector in relation to the displayed collision danger sectors the mariner can assess the risk of collision in multiple encounters and simultaneously identify feasible and precise course and/or speed evasive manoeuvres to avoid potential collision threats with a minimum safety distance.

The principal result of the simulator studies is that collision avoidance assessment based on the proposed visualisation-based collision avoidance display facilitates time-efficient and homogeneous decision-making and execution of precise and safe evasive manoeuvres. It appears likely that the need for long-term experience for correct assessment of the collision risk and evasive manoeuvres can be significantly reduced compared to conventional judgement techniques. The studies have also revealed the risk of temptation to make frequent and minor course alterations, which need to be emphasized in any training programme to avoid misjudgement and mistakes.

The superiority of the collision avoidance display increase with the excess speed of own ship, traffic density and complexity compared to ARPA (true and relative motion) displays. It appears particularly evident that HSC operating in congested waterways would receive the greatest benefits. Further work should focus on comparative studies that include the Trial Manoeuvre functionality on standard ARPA systems as well as the anti-collision information concepts Potential Point(s) of Collision (PPC) and Predicted Area of Danger (PAD). An appropriate target selection procedure is required to investigate in order to avoid or minimize the risk of an overloaded collision avoidance display in congested waterways. The easily understandable interpretation of collision risk to multiple targets and identification of feasible evasive action in true motion suggests that the proposed visualisation-based anti-collision display should have the potential to become widely accepted by mariners.

ACKNOWLEDGEMENTS

Sincere gratitude is expressed to Professor Dr. Kiyoshi Hara, President of Kobe University of Mercantile Marine, for inviting the first author to carry out this research. Sincere thanks are also expressed to the staffs of Professor Dr. Kinzo Inoue's Laboratory and Japan Marine Science Inc. whose administrative and technical assistance has been invaluable. The Captains of the NYK Line and from the company operating the K-Jet hydrofoil crafts and the students of Kobe University of Mercantile Marine that kindly participated in the simulator test programmes are very appreciated. Financial support for this research has been received from the Norwegian University of Science and Technology.

REFERENCES

Inoue, K. *et al.* (1998). Modelling of Mariners' Perception of Safety. *J. Japan Institute of Navigation*, **98**, 235–245.

Inoue, K. (2000). Evaluation Method of Ship-handling Difficulty for Navigation in Restricted and Congested Waterways. This *Journal*, **53**, 167–180.

https://doi.org/10.1017/S0373463303002388 Published online by Cambridge University Press

Lenart, A. S. (1983). Collision Threat Parameters for a new Radar Display and Plot Technique. This *Journal*, **36**, 404–410.

Pedersen, E., Inoue, K. and Tsugane, M. (2002a). Evaluation of a Radar Plot and Display Technique for Anti-collision Assessment of Multiple Targets in True Vector Representation by Application of the Environmental Stress Model. *J. Japan Institute of Navigation*, **106**, 1–12.

Pedersen, E., Inoue, K. and Tsugane, M. (2002b). On Decision Making in Connection with Optimal Anti-collision Manoeuvres by High Speed Craft in Waters Congested by Conventional Speed Vessels. *J. Japan Institute of Navigation*, **107**, 177–183.

Pedersen, E. and Jacobsen, A. (2002). On a Radar Plot and Display Technique for Judging Anti-collision Manoeuvres from the Viewpoint of Acquired Targets. *Singapore Maritime & Port Journal 2002*, 67–73, Maritime and Port Authority of Singapore.

https://doi.org/10.1017/S0373463303002388 Published online by Cambridge University Press